ELSEVIER

Physica A 313 (2002) 32–46

PHYSICA A

www.elsevier.com/locate/physa

Rough ideas on wetting

David Quéré

Laboratoire de Physique de la Matière Condensée, UMR 7125 du CNRS, Collège de France, 75231 Paris Cedex 05, France

Abstract

After a brief presentation of the classical laws of wetting, we review different phenomenological descriptions of rough wetting, i.e., show how these classical laws must be modified on rough solids. This introduces the questions of hemi-wicking (can a film propagate inside the texture of a solid?), rough films (is it possible for a liquid film to follow the roughness of a solid?) and super-hydrophobicity (how can a solid be designed to become water repellent?).

PACS: 68.10.−m; 68.45.Gd; 68.35.Ct

Keywords: Wetting; Impregnation; Thin films; Water repellency

1. Foundations

Two hundred years ago, Young [1] showed that the *contact angle* of a drop deposited on a solid is given by the relation

$$\cos\theta = \frac{\gamma_{SV} - \gamma_{SL}}{\gamma_{LV}}\,, \tag{1}$$

where γ_{IJ} is the surface tension (i.e., energy per unit surface) of the interface IJ, and the letters S, L, V designate the phases of the solid, liquid and vapor. A pedestrian derivation of Young's law consists in writing the surface energy of the drop as $E = \Sigma_{LV}\gamma_{LV} + \Sigma_{SL}\gamma_{SL} + (\Sigma_S - \Sigma_{SL})\gamma_{SV}$, where Σ_{IJ} is the surface area between phases I and J, and Σ_S the total surface of the solid. If the drop is small, gravity can be ignored, and the droplet is a spherical cap (Fig. 1), which yields simple formula for Σ_{LV} and Σ_{SL}. Minimizing E, keeping the drop volume constant leads to Eq. (1).

E-mail address: quere@ext.jussieu.fr (D. Quéré).

0378-4371/02/$ - see front matter
PII: S0378-4371(02)01033-6

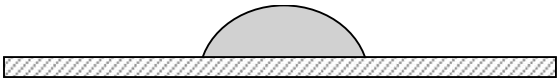

Fig. 1. Liquid droplet on a solid. The liquid joins the solid with an angle θ.

Young's derivation was much more straightforward. The contact angle is a local property which does not depend on the drop size, and which fixes in the vicinity of the *contact line*, where the three phases coexist. There, each surface tension acts to reduce the corresponding surface area. Balancing these three forces on the solid plane immediately gives Eq. (1).

Different remarks can be made, at this elementary level:

1. The surface forces could also have been projected on the vertical direction. We deduce that the liquid/vapor surface tension exerts all along the contact line a vertical force on the solid, which resists because of its elasticity. Roughly, Hooke's law indicates that the solid deformation should be of the order of γ_{LV}/E, where E is a Young's modulus of the solid. For hard solids, this deformation is non-observable, but it becomes appreciable for soft solids (like gels): a drop of water put on a fresh paint, after it evaporates, indeed leaves a circular ridge on the paint.
2. For tiny drops, the energy of the line, or *line tension* T, may be considered [2]. This induces a correction of the contact angle which increases as the ratio length/surface increases. The correction should be of the order of $T/\gamma r$, noting r the size of the drop. T/γ is expected to be of the order of 1 nm, so that this effect should be negligible for drops larger than 1 μm. Many contradictory experimental results coexist on this subject, maybe due to ill-adapted optical techniques [3], but recent AFM measurements seem to clarify the picture [4].
3. The different surface tensions in Eq. (1) have values typically between 20 and 1000 mN/m. There is no theorem forcing the ratio $(\gamma_{SV} - \gamma_{SL})/\gamma_{LV}$ to be smaller than unity (in absolute value). These cases appear to be particularly interesting practically:

   (A) If $(\gamma_{SV} - \gamma_{SL})$ is larger than γ_{LV}, the drop tends to spread completely on the solid ($\theta = 0$). Silicone oil on most solids (glass, or steel, or even plastics) realizes such a *complete wetting*. Conversely, a liquid film coating a solid will be stable if the same inequality is satisfied. This explains why liquids of low surface tension (such as silicone oils) wet most surfaces. For this reason, surfactants, which lower the liquid/vapor surface tension, will be often added to a paint to make it wetting. More generally, the questions of the transitions between partial and complete wetting have been studied quite extensively, together with precise descriptions of microscopic films which develop in the regime of complete wetting [5–7].

   (B) If $(\gamma_{SL} - \gamma_{SV})$ is larger than γ_{LV}, the drop should be in a pure drying situation, sitting on the solid as a marble ($\theta = 180^\circ$). But it turns out that there is no physical system which realizes such a situation. For example, water on solids of

very low wettability (such as fluorinated solids) makes contact angle of the order of 120° or 130°, quite far from the ultimate value of 180° [8]. Nevertheless, a very simple way to observe a non-wetting situation consists of inverting the liquid and vapor phases: then, the contact angle is $\pi - \theta$, which leads to a "drying" situation (for the vapor) for $\theta = 0$: a bubble of air rising in a box filled with a silicone oil reaches the top of the box with a contact angle of 180°. One of our aims in this paper will be to show how drying situations can be approached for liquids, using tricky solids.

4. The criterion for complete wetting ($\gamma_{SV} - \gamma_{SL} > \gamma_{LV}$) is much more difficult to satisfy than the one for impregnation: the condition for filling spontaneously a little tube put in contact with a reservoir is a solid/liquid surface of lower energy than the solid/vapor one, i.e., $\gamma_{SV} > \gamma_{SL}$. In terms of contact angle, wetting occurs when the contact angle goes to zero, while impregnation takes place when it is smaller than 90°. The latter condition is extremely common, and this explains why most liquids invade most sponges (or papers, or soils), although generally liquids do not spread on solids: impregnation just implies to replace one surface by another one, while wetting imposes to replace one by two. Another aim here is to describe an intermediate case, so-called rough wetting, which concerns the behavior of a liquid on a rough surface, which can be seen as a kind of 2d porous medium.

2. More real surfaces

Wetting in reality turns out to be much more complex than described above. This primarily comes from the non-ideality of solid substrates which are both rough and chemically heterogeneous. (Liquid drops can also be non-ideal, containing different chemical species as surfactants, or other solid or liquid phases—this also modifies the picture, but we will not describe here this emergent field.) Very simple observations reveal this non-ideality: for example, little droplets generally remain stuck on a tilted substrate (on vertical windows, for example). This proves that, though the drop is static, different angles can coexist along the contact line: large ones at the front of the drop, and smaller at the rear—which generates a capillary force which is able to balance the weight for small drops [9]. This phenomenon, known as the *hysteresis of the contact angle*, is a difficult question of statistical physics which has attracted many efforts in the last two decades [5].

It is not our purpose here to describe this subject, but it is worth stressing how a unique defect can induce a variability in the contact angle. This is quite obvious for a chemical discontinuity at the surface: supposing a substrate where the contact angle is θ_1 on one side and θ_2 on the other side, the contact angle can fluctuate between these two values at the frontier between both sides. It is also true for a discontinuity of the solid slope (Fig. 2). Supposing the defect microscopic, so that the angles are measured taking the horizontal as a reference, the angle can vary at the edge point between θ, the Young contact angle, and $\pi - \Psi - \theta$. This variation can be very large: at the top of a water glass, we can see the angle varying between 0° (water wets the glass)

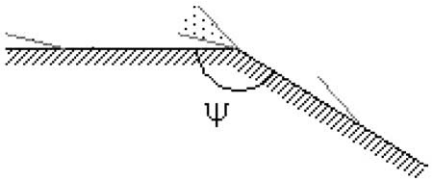

Fig. 2. On a sharp edge, the contact angle (represented before and after the defect) can fluctuate, as indicated.

and 180° (since we have at this particular point $\Psi = 0$), where the latter case defines an over-filled glass.

Thus, defects on a solid surface can induce fluctuations of the contact angle (we note $\Delta\theta$ the amplitude of this fluctuation). But they can also modify the value of the effective contact angle observed on the substrate. The data of Johnson and Dettre [10] reported in Fig. 3 show the advancing θ_a (maximum static angle) and receding θ_r (minimum static angle) contact angles of water on surfaces of wax of variable roughness.

As the roughness (defined here only qualitatively) increases, we first notice small variations of the angles, together with a significant increase of the hysteresis. Then, both angles suddenly increase while the hysteresis nearly vanishes. Hence, texturing a solid does not only modify the hysteresis: it can also affect dramatically the value of the mean contact angle itself. Interestingly, the effects reported in Fig. 3 correspond to a given surface chemistry, i.e., fixing the Young contact angle θ: for water on wax, θ is of the order of 110°, while the effective contact angle θ^* in the regime of large roughness jumps to $\theta^* \approx 160^\circ$.

The contact angle can also be tuned by the solid roughness in the hydrophilic region ($\theta < 90^\circ$), as shown by Shibuichi et al. [11]. Their data are summarized in Fig. 4, where the effective contact angle on a rough surface is plotted versus the Young contact angle (the data are obtained by varying the liquid on a given rough or flat substrate).

There again, the roughness is observed to affect dramatically the contact angle, but differently according to the wettability region. In the hydrophilic domain ($\cos\theta > 0$), the effective contact angle is found to be smaller than the Young angle ($\theta^* < \theta$). In the hydrophobic side ($\cos\theta < 0$), it is the contrary: as in Fig. 3, the contact angle is observed to increase largely ($\theta^* > \theta$), if the substrate is rough enough.

A phenomenological model was proposed long ago by Wenzel [12], for understanding how roughness affects wetting. Let us consider a rough solid, with a roughness parameter r defined as the surface area of this solid normalized by its apparent surface area (the roughness scale is taken small, so that the solid is apparently smooth). The effective contact angle on this surface is evaluated by considering a small displacement dx of the contact line, as pictured in Fig. 5.

This displacement implies a change in surface energy (per unit length of the contact line):

$$dE = r(\gamma_{SL} - \gamma_{SV})\,dx + \gamma_{LV}\,dx\cos\theta^*, \tag{2}$$

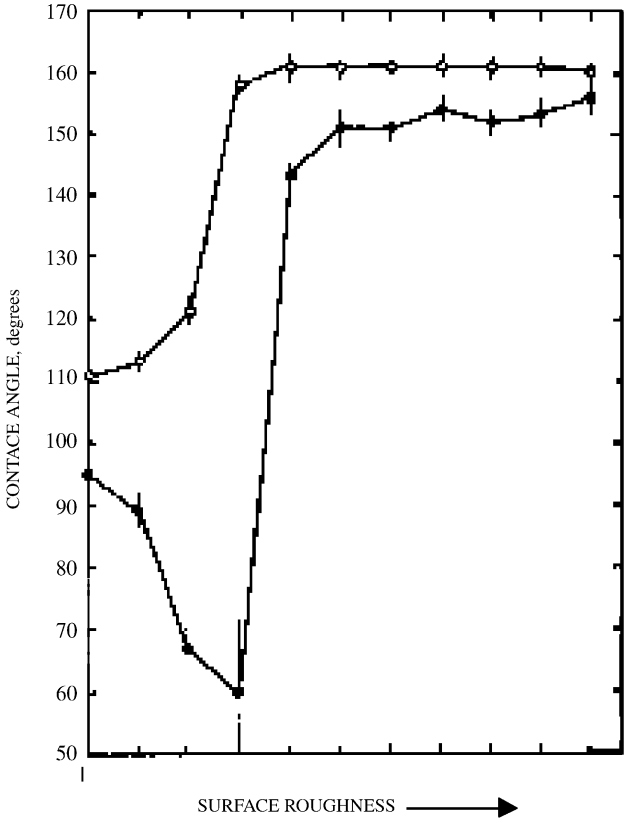

Fig. 3. Static contact angle of water on wax substrates, as a function of the substrate roughness. Both the advancing angle (open symbols) and the receding ones (full symbols) are displayed (from Johnson and Dettre [10]).

E is minimal at equilibrium. For $r = 1$ (flat solid), we deduce Young's equation (Eq. (1)). For a rough surface, we derive Wenzel's relation (for a recent analysis see also [13]):

$$\cos\theta^* = r\cos\theta\,, \tag{3}$$

where θ is Young's angle. This very compact relation predicts: $\theta^* < \theta < 90^\circ$ and $\theta^* > \theta > 90^\circ$ (since we have $r > 1$). Both hydrophobicity and hydrophilicity are reinforced by roughness, in qualitative agreement with the different behaviors shown in Figs. 3 and 4. But this agreement is only qualitative: we do not observe a simple linear relation in Fig. 4, and do not understand the discontinuity in contact angle found in Fig. 3. We discuss different scenarios for explaining these discrepancies.

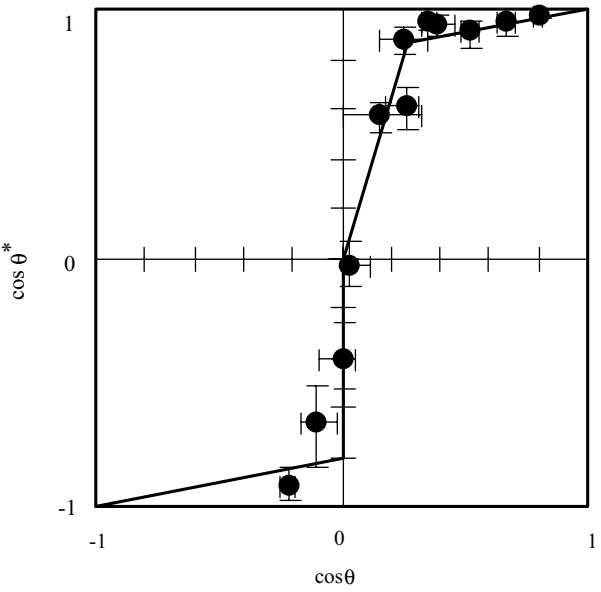

Fig. 4. Cosine of the effective contact angle θ^*, as a function of the cosine of the Young angle θ (determined on a flat surface of the same material and varied using different liquids). The thin straight lines (from left to right) are, respectively, Eqs. (11), (3) and (8) (Shibuichi et al. [11]).

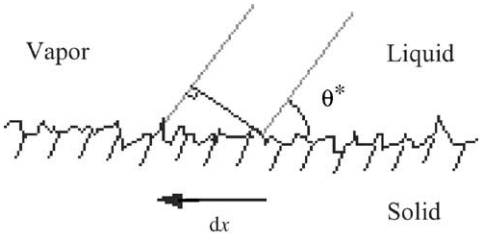

Fig. 5. The Wenzel picture: the effective contact angle θ^* is obtained by considering a small apparent displacement of the contact line.

3. From hemi-wicking to rough films

A rough (or textured) surface is a kind of 2d porous medium, likely to be invaded by a liquid. When a drop is brought in contact with the solid, we can imagine that a film propagates inside the roughness, so that the drop eventually coexists with this film. What is the condition for such a propagation?

Let us consider for the sake of simplicity a solid textured with a "two-stages" design, as sketched in Fig. 6: a flat bottom, upon which isolated spikes (or ridges) are deposited. We note ϕ_S the surface area of the second stage (i.e., the top of the

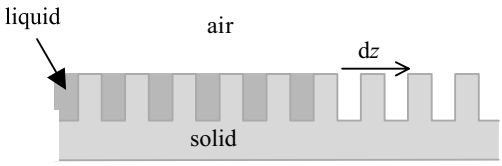

Fig. 6. Liquid film propagating in geometric textures on a solid.

spikes, or the top of the ridges) normalized by the total surface area of the sample ($\phi_S < 1$). Let us put such a sample in contact with a liquid, and suppose that the liquid has risen up to a height z. For a further displacement by a quantity dz, the surface energy changes by

$$dE = (\gamma_{SL} - \gamma_{SV})(r - \phi_S)\,dz + \gamma_{LV}(1 - \phi_S)\,dz\,, \tag{4}$$

where the first term expresses that liquid wets the inside of the texture, but not the top (we suppose that the wetting is partial), and the second one the fact that the progression of this film implies the development of a liquid/vapor interface. (This justifies the term of *hemi-wicking*.) The energy decreases if the Young angle verifies the condition [14]:

$$\theta < \theta_c \quad \text{with} \quad \cos\theta_c = \frac{1 - \phi_S}{r - \phi_S}\,. \tag{5}$$

We can notice that Eq. (5) indeed defines a cosine, whatever the design of the substrate. In particular, for flat surfaces ($r = 1$), we find that the liquid invades the substrate if its contact angle vanishes ($\theta_c = 0$). For porous media ($r = \infty$), we recover the classical criterion of impregnation stressed in the first section ($\theta_c = 90^\circ$). For textured surfaces, the criterion is intermediate between these two cases, since θ_c is expected from Eq. (5) to be intermediate between 0° and 90° (logically, since hemi-wicking is itself intermediate between complete wetting and usual wicking). We also deduce from Eq. (4) the driving force (per unit length) of the film, which is dE/dz. If the viscous friction is dominant (compared with the liquid inertia), and thus of the form $\eta V z$, where V is the film velocity and η the liquid viscosity, we expect the film progression to follow a diffusive-type law ($z \sim \sqrt{t}$, with t the time). This law is quite general in impregnation processes, and often called the Washburn law [15].

The second regime in Fig. 3 can be interpreted as resulting from the progression of such a film. Then, the drop lies on a mixture of liquid (which constitutes the film) and solid (the "islands" which emerge above the sea of liquid). The contact angle of such a drop can be deduced from an argument due to Cassie and Baxter [16]. If we suppose, quite generally, that a drop sits on a patchwork of (small) domains 1 (with a probability f_1) and 2 (with a probability f_2), then displacing the contact line by a quantity dx changes the surface energies by

$$dE = [f_1(\gamma_{SL} - \gamma_{SV})_1 + f_2(\gamma_{SL} - \gamma_{SV})_2]\,dx + \gamma_{LV}\,dx\cos\theta^*\,. \tag{6}$$

At equilibrium ($dE = 0$), we deduce that the effective contact angle obeys the relation

$$\cos\theta^* = f_1\cos\theta_1 + f_2\cos\theta_2\,, \tag{7}$$

where θ_1 and θ_2 are the Young contact angles on large domains of 1 and 2, respectively. For drop coexisting with a film impregnating the solid texture, we have $f_1 = \phi_S$, $\theta_1 = \theta$, $f_2 = 1 - \phi_S$ and $\theta_2 = 0$, so that we expect the effective contact angle to be given by the relation [14]

$$\cos\theta^* = (1 - \phi_S) + \phi_S \cos\theta \,. \tag{8}$$

This relation is in fair agreement with the data in Fig. 3. It shows that hemi-wicking improves the solid wettability ($\theta^* < \theta$), but less efficiently than with the Wenzel scenario: for $\theta < \theta_c$, the angle deduced from Eq. (8) is larger than the one derived from Eq. (3). This can be understood as due to a "smoothing" effect of the film, which erases the solid roughness and thus prevents the Wenzel effect to take place. In addition, Eq. (8) predicts that it is not possible to induce a wetting transition ($\theta^* = 0$) by texturing a solid. This result is in contradiction with a recent model by Netz and Andelman [17], which could be simply due to the hypothesis, in the latter model, that solid and liquid interfaces cannot cross.

This phenomenological description of the wetting of a rough surface may be useful, but different questions would deserve a more complete approach. One of the main issues, for example, concerns a surface of any roughness (such as sketched in Fig. 5). Eqs. (5) and (8) should remain valid, but the fraction ϕ_S, which is defined by the surface area of the emerged island, is unknown. It would be worth generalizing the model for such disordered surfaces. Another question is the determination of the contact angle hysteresis on these surfaces. We derived equations for an effective angle, but did not say anything about the fluctuations of this angle. The situation should be different according to the value of θ. For $\theta > \theta_c$ (see Eq. (5)), we should be in the usual situation of a large contact angle hysteresis due to the multiple defects on the surface. For $\theta < \theta_c$ (hemi-wicking), we can guess that the receding angle should be zero (the drop coexisting with a film of same liquid), while the value of the advancing angle should be close to the one proposed in Eq. (8). These surfaces should thus exhibit a non-negligible contact angle hysteresis.

Another question of interest is the case of complete wetting ($\theta = 0$). Then, a film should develop from the drop and progress quicker than on a flat surface, because of the accidents of the surface (we emphasized that this led to a law for the progression of the film in $t^{1/2}$, instead of $t^{1/10}$ for the radius of a spreading drop on a flat surface). But the islands should be themselves covered by a microscopic wetting film. This phenomenon should be quasi-instantaneous, using hemi-wicking as a reservoir. The film can also be forced by coating processes, which raises the question of its own roughness: does it follow the solid roughness as sketched in Fig. 7 or can it smoothe it [18]? If the film were a monolayer (thickness a, i.e., the size of the molecule), the answer would be that the film follows the roughness (except at the microscopic scale a), so that the film would have the same roughness as the solid.

But it turns out that very frequently, the long-range forces through a microscopic wetting film cannot be neglected. Van der Waals forces, for example, often favor films thicker than a, and the intermolecular potential related to these forces can be written (per unit surface) $W(h) = -A/12\pi h^2$, where h is the film thickness and A the Hamaker constant of the system (A is related to the contrast in polarizability between the different

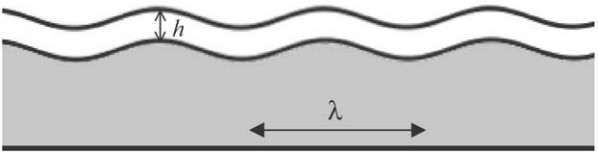

Fig. 7. The coating of a rough solid by a liquid can preserve the roughness if the film is thin enough (see below).

phases). A is positive in our case, which means that this potential indeed favors thick films (but of course thinner than the range of van der Waals forces, i.e., typically 100 nm) [5].

The physical ingredients of the problem are now identified: on the one hand, the long-range forces favor a thick film, and thus we expect a film of constant thickness thicker than the molecule size. On the other hand, surface tension opposes the formation of a rough film, and rather favors a smooth film, of smaller surface area. We note the modulations of the surfaces u_S and u_L, for the solid and for the liquid, respectively. The local film thickness is $h+u_L-u_S$, and the energy of the film can be written [3,18]

$$E=\int \mathrm{d}\Sigma \left[W(h+u_L-u_S)+\frac{1}{2}\gamma_{LV}(\nabla u_L)^2\right] , \tag{9}$$

where the second term is the excess in surface energy associated with a smooth modulation of the liquid/vapor interface. For small deformations, W can be expanded at the second order (for a film of constant thickness, $\langle u_L-u_S\rangle$ is zero). Minimizing E, we get an equation for the optimum profile of the liquid interface: $(u_L-u_S)\ W''(h)=\gamma_{LV}\Delta u_L$. For van der Waals forces, and noting $a=(A/2\pi\gamma)^{1/2}$, where a is typically 1 Å, it is written

$$u_L-\frac{h^4}{a^2}\Delta u_L=u_S . \tag{10}$$

The length $\xi=h^2/a$ finally allows us to classify the different solutions of Eq. (10) [18]. If the characteristic scale λ of modulation of the solid is larger than ξ, the modulation of the liquid surface is also of large wavelength so that Eq. (10) reduces to $u_L=u_S$. The film then follows the solid roughness. If on the contrary we have $\lambda<\xi$, then the surface term dominates and we expect $u_L=0$: the liquid surface is flat. Note that the length ξ can be typically between 10 nm (for $h=1$ nm) and 100 μm (for $h=100$ nm), which finally allows to tune this length, according to the desired purpose. For treating a rough solid to make it hydrophobic while keeping the roughness (the subject of the following section), we must take h of the order of 1 nm (monomolecular layer). On the other hand, to smoothe a rough solid (for optical purposes, for example: think about a hair that one would like to make shiny), h must be chosen to satisfy the condition $\lambda<\xi$, which yields typically $h=10$ nm taking $\lambda=1$ μm (a very typical value).

4. Pearl drops

We now examine the case of hydrophobic rough substrates. Then, as seen in Figs. 3 and 4, the hydrophobicity can be reinforced by the roughness, leading to super-hydrophobic substrates (effective contact angle θ^* typically larger than 160°) [19]. Wenzel's equation indeed predicts such a behavior, but the observations are not in quantitative agreement with this relation. In particular, it does explain the discontinuity in contact angle, and shows that drying transitions ($\theta^* = 180^\circ$) are likely to be induced (for $\cos\theta < -1/r$), which is not the case.

Another scenario may explain the super-hydrophobic state. A liquid deposited on a rough hydrophobic state should not necessarily follow the accidents of the solid surface. Instead, air could be trapped below the drop, which then sits on a patchwork of solid and air [10,20]. The more aerated the solid, the higher the contact angle (if the Solid tends towards the Vapor in Eq. (1), the contact angle tends towards 180°): many pieces of liquid/vapor should be created below the drop (with an energetic price to pay for each of them), and many contact lines. The condition of equilibrium for these contact lines is the Young condition, with $\theta > 90^\circ$ in this case. If the solid is rough enough, such a condition can be fulfilled thanks to the high slopes which develop locally, allowing the liquid/vapor surface to meet the solid with the prescribed angle. Thus, we understand qualitatively in Fig. 3 the existence of a threshold in roughness above which air trapping occurs, provoking a discontinuous increase of the contact angle.

A super-hydrophobic state can also occur on hydrophobic surfaces with a well-controlled design. Spikes, or crenellations, or even thin stripes, lead to such a state, because of their edges which allow the pinning of the contact line, as stressed in Fig. 2, and thus the entrapment of air. Many natural materials are super-hydrophobic, and indeed exhibit at the scale of typically 1–10 μm textures on their surfaces [21]. We can cite butterflies (for which the texture also provides the beautiful colors—remember that lepidopter means scaled wings), duck feathers and many plants, as lotus, gingko biloba, young pea or corn leaves, etc.

Fig. 8 shows a microphotograph of a lotus leaf, and as for most of these natural materials, we can notice two different scales of roughness (in this case, one around 10 μm, and the other below 1 μm). This is not understood. Of course, mixing two scales increases the super-hydrophobicity [22]. But the reason could be different: one possibility could be that for a roughness at a very small scale (smaller than 100 nm), van der Waals forces could force a contact between the solid and the liquid, which would make a Wenzel scenario at this scale, which would combine with the air pocket model at a larger scale (and of course confer a very high degree of hydrophobicity to the substrate). Another possibility could be that two scales of roughness could be adapted to get rid of two scales of drop sizes: typically rain and dew. It must finally be stressed that some animals (at least a Namibian beetle living in the desert) seem to mix hydrophilic regions with hydrophobic ones: the first kind to trap water, the second one to drive drops towards the animal's mouth [23].

The contact angle on a substrate favoring the air trapping can be evaluated as previously. Eq. (7) is used once again, with $f_1 = \phi_S$ (which defines the fraction of solid

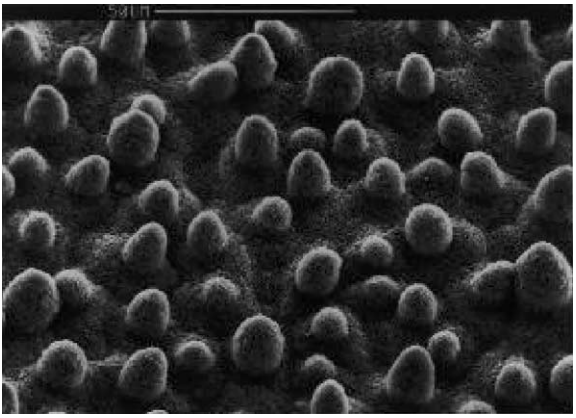

Fig. 8. Microphotograph of a lotus leaf, showing the textures responsible for the water-repellent character of these plants. The white bar on the top is 50 μm (courtesy of Wilhelm Barthlott).

remaining in contact with the drop), $\theta_1 = \theta$, and $f_2 = 1 - \phi_S$ and $\theta_2 = \pi$ (the "contact angle" of drop on air). This gives for the effective contact angle [20]:

$$\cos\theta^* = -1 + \phi_S(\cos\theta + 1)\,. \tag{11}$$

This formula predicts quite large values for the contact angle: with θ of about 120° and ϕ_S between 5% and 10%, we get effective contact angles around 170°. It is worth discussing if the system lowers its energy by trapping air below the drop, instead of having a solid/liquid interface following the solid texture (Wenzel model). If we compare the energy gained by displacing the contact line by a small quantity, we find that the energy is lower in the Wenzel situation if the Young contact angle is between 90° and an angle $\theta_d = \pi - \theta_c$, where θ_c is defined by Eq. (5). Thus, in most cases, the air trapping regime should be metastable [24]. This could come from the difficulty to evacuate air when depositing a drop on such rough solids. It could be interesting to prove this fact by comparing what happens when depositing a drop and when building it by vapor condensation; in the latter case, the contact angle should be rather given by Wenzel's relation, and thus observed to be smaller than the one observed in a deposition process (Eq. (11)).

There again, we did not discuss the value of the contact angle hysteresis. In Fig. 3, it is observed that it becomes very small once air is trapped (which provokes the simultaneous jump of both the receding and the advancing angles). This can be qualitatively understood by considering that air below the drop "homogenezes" the substrate, which is almost air with a little fraction of solid. A more quantitative analysis of this remarkable phenomenon remains to be done, but let us stress a very practical consequence: on such an inclined solid, droplets do not stick, as they do usually.

This point is worth being developed. A drop usually sticks on a solid (even tilted) because of the contact angle hysteresis. If we write that half the drop joins the solid (at the rear) with an angle $\theta_r = \bar{\theta} - \Delta\theta/2$, and that the other half (at the front) joins it with an angle $\theta_a = \bar{\theta} + \Delta\theta/2$ ($\bar{\theta}$ is a mean contact angle), we can calculate the

capillary force. It can be written $\pi b\gamma_{LV}(\cos\theta_r - \cos\theta_a)$, where b is the radius of the solid/liquid contact (quasi-circular for $\Delta\theta \ll \bar{\theta}$). In the limit of large contact angles (we write $\bar{\theta} = \pi - \varepsilon$) and small hysteresis, this force reduces to $\pi b\gamma_{LV}\varepsilon\Delta\theta$, and indeed vanishes quickly.

Then, an interesting question is the size b of the contact. There again, the answer is different from the usual situation, for which b is easily deduced from geometry, and found to vary linearly with the size R of the drop. Mahadevan and Pomeau [25] showed that for a drop in a non-wetting situation, the contact mainly comes from the drop weight. Supposing that the drop center of mass is lowered by a quantity δ, the capillary force tending to restore the spherical shape can be written (dimensionally) $\gamma\delta$, while the drop weight is (again, dimensionally) $\rho g R^3$. The balance of these forces, together with the geometric relation $b^2 \sim \delta R$, yields [25]:

$$b \sim R^2\kappa\,, \tag{12}$$

where κ^{-1} is the capillary length ($\kappa^{-1} = (\gamma_{LV}/\rho g)^{1/2}$, where ρ is the liquid density, κ^{-1} is 2.7 mm for water). The size of the contact is therefore found to be quadratic in the drop size, instead of linear as it is usually for drops.

The drop is stuck if the capillary force, which opposes the weight, is larger than the weight of the drop. In the limit we considered, this condition gives for the maximum size of a stuck drop on a vertical plate ($\alpha = 90^\circ$):

$$R \sim \varepsilon\Delta\theta\kappa^{-1}\,. \tag{13}$$

Usually, drops smaller than the capillary length get stuck, and larger ones move (one can check that looking at the window on a rainy day). But we find here that in a super-hydrophobic situation, this threshold can be reduced dramatically, by a factor $\varepsilon\Delta\theta$ (where both angles are expressed in radians; this factor can typically be between 0.1 and 0.01). This has an interesting consequence: since drops run down on this kind of substrate, they clean it by passing. This is sometimes called the lotus effect, or (improperly) self-cleaning effect, and different materials are now available with (pretended) such properties. Aging should be a problem for these artificial materials, which do not renew their surfaces as plants do: a super-hydrophobic solid is likely to be also a super-lipophilic material, and thus to see its cavities filled with oils as time goes on. It is also fragile, and the roughness can be damaged by mechanical operations.

There is another way which allows to reach the limit of hydrophobicity, namely a contact angle of 180°. It consists of treating the liquid/vapor interface instead of the solid one. Mixing a powder of hydrophobic materials (such as soot, or silica grains treated with fluorosilanes) with water leads to an encapsulated drop of water: the grains coat the droplet, producing a so-called *liquid marble* which does not wet the substrate on which it is deposited, whatever its nature [26]. Simplifying the grains as small cubes, and comparing the energy of system grain/interface before and after placing one side of the grain at the interface, we obtain per unit area and per grain: $\gamma_{SL} - \gamma_{LV} - \gamma_{SV} = -\gamma_{LV}(1+\cos\theta)$ (noting θ the Young angle of the liquid on the material constituting the grain), which is indeed negative. In addition, the grain is stuck at the interface (and does not sink inside the drop) because of its hydrophobicity. These

Fig. 9. Millimetric marble of water coated with a hydrophobic powder floating on water (courtesy Pascale Aussillous).

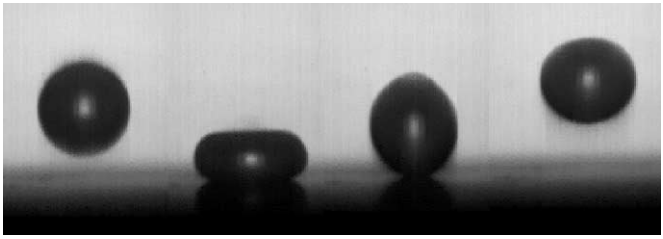

Fig. 10. Millimetric water-drop crashing and bouncing on a super-hydrophobic solid (courtesy of Denis Richard).

marbles are waterproof enough to be able to float at the surface of water, as observed in Fig. 9.

On a dynamic point of view, these different kinds of liquid balls have remarkable properties. Because of the very small contact (see Eq. (12)), the friction is highly reduced and the droplets are very quickly evacuated. The motion can induce changes in shape: a spherical marble was observed to transform as it runs down in a peanut or in a doughnut, which reveals a rotation of the drop as it moves [26]. Another property is the ability of these drops to bounce when they are thrown on the solids [27,28]. This is quite unusual: a drop crashing on a solid generally spreads because of its inertia and slightly retracts to reach its static contact angle. The kinetic energy is burnt by viscosity (in particular close to the advancing moving contact lines, where velocity gradients can be very large), and the drop quickly stops. Of course, our common experience tells us that this is generally complicated by epiphenomena, such as splashes or even (on hydrophobic materials) a partial rebound.

The situation is quite different with pearl drops. A full rebound can be observed, as reported in Fig. 10, where four successive snapshots show a bouncing sequence. The drop crashes, but the dynamic contact angle remains stuck to its maximum value (180°): moving contact lines are suppressed, which highly reduces the viscous dissipation. In addition, the drop which is in non-wetting situation, stores its kinetic energy in surface

energy, which allows the rebound. The velocity of impact in Fig. 10 is such that the kinetic and surface energies of the impacting drop are the same (the ratio between both quantities defines a dimensionless number, the Weber number). We indeed observe a significant maximum deformation, of the order of the drop size.

Many questions can be raised about this phenomenon of capillary elasticity, which justifies that these surfaces are often referred to as water-repellent. For example, the restitution coefficient of the shock can be very high, of the order of 0.9. Moreover, this quantity critically falls down to zero at small impact velocity (typically 5 cm/s), indicating a transition towards sticking [28]. Both these behaviors remain to be quantitatively understood. More generally, we all know that a drop does not usually bounce, and the way the bouncing sets up as a function of the contact angle should be established. This is of obvious practical interest, and would help to define more precisely a criterion of water-repellency.

5. Conclusions

The bouncing drop in Fig. 10 can be seen as a metaphor of wetting. Although identified since 200 years, wetting still lives and bounces constantly thanks to new questions—often arising from practical considerations. We tried here to show how the classical laws of wetting can be adapted to real surfaces, restricting the word "real" to "rough". We stressed in particular the case of rough hydrophobic substrates which allow to achieve water-repellent materials. More generally, great progress was made in the achievement of well-controlled microstructures on solid surfaces, thanks to techniques from micro-electronics, which led to the renewal of this field in the last few years.

A second important family of real substrates concerns surfaces which are heterogeneous chemically. There again, we can distinguish disordered surfaces from surfaces with well-designed patterns. The Cassie–Baxter model (Eq. (6)) is a first approach to characterizing the wettability of these surfaces, but many questions remain such as the value of the contact angle hysteresis (for which interesting numerical approaches were recently proposed [29]), or the shape and roughness of the contact line [3,30,31]. As for rough substrates, these questions are stimulated by the recent progress which was made in the achievement and characterization of such surfaces.

Another class of problems concerns the local behavior of liquids on textured surfaces. We considered all along this review drops much larger than the size of the defects (which allowed average calculations). But in some cases, the typical size of the drop can be comparable with the size of the pattern: we can think of dew on micrometric defects, or on liquid ridges on stripes, as developed for microfluidics devices. The latter situation takes advantage of the chemical discontinuity on the edges on the stripe, which permits the pinning of the contact line and thus of the ridge along the stripe. Much progress was made recently on these systems, in particular, the findings of morphological transitions as a function of the quantity of liquid injected along a given pattern: let us quote for example the appearance of bulges (whose shape reminds onduloidal drops on fibers) for over-fed stripes [32]. A recent and comprehensive

review on this subject is due to Lipowsky [33], where the interested reader will find many complements to this study.

Acknowledgements

It is a pleasure to thank José Bico for his contribution in this field. In addition, I thank Pascale Aussillous, Wilhelm Barthlott, Christophe Clanet, Pierre-Gilles de Gennes, Stephan Herminghaus, Aurélie Lafuma, Christian Marzolin, Christoph Neinhuis, Denis Richard and Christophe Tordeux for many valuable discussions, encouragement or collaborations.

References

[1] T. Young, Philos. Trans. R. Soc. London 95 (1805) 65.
[2] J. Rowlinson, B. Widom, Molecular Theory of Capillarity, Oxford University Press, Oxford, 1982.
[3] P.G. de Gennes, F. Brochard-Wyart, D. Quéré, Bulles, gouttes, perles et ondes, Belin, Paris, 2002.
[4] T. Pompe, S. Herminghaus, Phys. Rev. Lett. 85 (2000) 1930–1933.
[5] P.G. de Gennes, Rev. Mod. Phys. 57 (1985) 827–863.
[6] A.M. Cazabat, Adv. Colloid Interface Sci. 42 (1992) 65–87.
[7] D. Bonn, D. Ross, Rep. Prog. Phys. 64 (2001) 1085–1163.
[8] E.G. Shafrin, W.A. Zisman, Contact angle, wettability and adhesion, Adv. Chem. Ser. 43 (1964) 145–157.
[9] E.B. Dussan, R.T.P. Chow, J. Fluid Mech. 137 (1983) 1–29.
[10] R.E. Johnson, R.H. Dettre, Contact angle, wettability and adhesion, Adv. Chem. Ser. 43 (1964) 112–135.
[11] S. Shibuichi, T. Onda, N. Satoh, K. Tsujii, J. Phys. Chem. 100 (1996) 19512–19517.
[12] R.N. Wenzel, Ind. Eng. Chem. 28 (1936) 988–994.
[13] P.S. Swain, R. Lipowsky, Langmuir 14 (1998) 6772–6780.
[14] J. Bico, C. Tordeux, D. Quéré, Europhys. Lett. 55 (2001) 214–220.
[15] E.W. Washburn, Phys. Rev. 17 (1921) 273–283.
[16] A.B.D. Cassie, S. Baxter, Trans. Faraday Soc. 40 (1944) 546.
[17] R.R. Netz, D. Andelman, Phys. Rev. E 55 (1997) 687–700.
[18] D. Andelman, J.F. Joanny, M.O. Robbins, Europhys. Lett. 7 (1988) 731–736.
[19] T. Onda, S. Shibuichi, N. Satoh, K. Tsujii, Langmuir 12 (1996) 2125–2127.
[20] J. Bico, C. Marzolin, D. Quéré, Europhys. Lett. 47 (1999) 220–226.
[21] C. Neinhuis, W. Barthlott, Ann. Bot. 79 (1997) 667–677.
[22] S. Herminghaus, Europhys. Lett. 52 (2000) 165–170.
[23] A.R. Parker, C.R. Lawrence, Nature 414 (2001) 33–34.
[24] J. Bico, U. Thiele, D. Quéré, Colloids Surf. A (2002) to be published.
[25] L. Mahadevan, Y. Pomeau, Phys. Fluids 11 (1999) 2449–2453.
[26] P. Aussillous, D. Quéré, Nature 411 (2001) 924–927.
[27] G.S. Hartley, R.T. Brunskill, in: J.F. Danielli (Ed.), Surface Phenomena in Chemistry and Biology, Pergamon Press, London, 1958, pp. 214–223.
[28] D. Richard, D. Quéré, Europhys. Lett. 50 (2000) 769–775.
[29] S. Brandon, A. Wachs, A. Marmur, J. Colloid Interface Sci. 191 (1997) 110–116.
[30] E. Decker, S. Garoff, Langmuir 13 (1997) 6321.
[31] E. Rolley, C. Guthman, R. Gombrovicz, V. Repain, Phys. Rev. Lett. 80 (1998) 2865.
[32] H. Gau, S. Herminghaus, P. Lenz, R. Lipowsky, Science 283 (1999) 46–49.
[33] R. Lipowsky, Curr. Opinion Colloid Interface Sci. 6 (2001) 40–48.